TECHNICAL MEMORANDUMS

NATIONAL ADVISORY COMMITTEE FOR AERONAUTICS

No. 768

THE INTERDEPENDENCE OF PROFILE DRAG AND LIFT WITH JOUKOWSKI TYPE AND RELATED AIRFOILS

By H. Muttray

Luftfahrtforschung
Vol. 11, No. 6, December 5, 1934
Verlag von R. Oldenbourg, München und Berlin

1.1
1.2.1.1

Washington
March 1935

NATIONAL ADVISORY COMMITTEE FOR AERONAUTICS

TECHNICAL MEMORANDUM NO. 768

THE INTERDEPENDENCE OF PROFILE DRAG AND LIFT WITH JOUKOWSKI TYPE AND RELATED AIRFOILS*

By H. Muttray

SUMMARY

On the basis of a systematic investigation of Göttingen wind-tunnel data on Joukowski type and related airfoils, it is shown in what manner the profile drag coefficient is dependent on the lift coefficient. It is found that, up to camber parameters $\frac{f}{l} = 0.25$ and thickness parameters $\frac{d}{l} = 0.4$, the profile drag coefficient is represented as a cubical parabola whose apex for cambered airfoils with c_a values lies above zero. With given camber these peak c_a values are in approximately linear relationship with the thickness parameters. The individual factors for the construction of the profile drag polars are given. They afford a more accurate calculation of the performance coefficients of airplane designs than otherwise attainable with the conventional assumption of constant profile drag coefficient.

1. INTRODUCTION

The assumption of constant parasite drag coefficient in the performance calculation of airplane designs (reference 1) is particularly inadequate when the c_a values are high, because a portion of this drag, the so-called "profile drag",** upon approaching $c_a = 1.0$, rises considerably with increasing c_a values. As a result the aero-

*"Über die Abhängigkeit des Profilwiderstandes vom Auftrieb bei Joukowsky- und joukowsky-ähnlichen Profilen." Luftfahrtforschung, December 5, 1934, pp. 165-173.

**The presumption of constant coefficient of residual drag (body drag and protruding parts) is preserved.

dynamic characteristics, such as criterion of climb and lift/drag ratio, approach for flight with best climb and ceiling factor rather the values for flight with best fine-fineness ratio, and consequently do not reach the figures arrived at with an assumedly constant parasite drag coefficient.

However, since this assumption results in a comparatively convenient method of calculation, it was attempted to extend these methods at least to a group of such wing sections for which the assumption of constant parasite drag coefficient does no longer hold. To this end, we introduced in Schrenk's report (reference 2) a second law for the quantity of the profile drag coefficient as function of c_a, to which the representation of the profile drag polars as a parabola symmetrical to the c_w axis corresponded. Then the profile drag is:

$$c_{w_{profile}} = c_{w_{profile_{min}}} + \text{constant } c_a^2 \qquad (1)$$

In this manner the profile drag coefficient consists of a part independent of c_a and a part dependent on c_a squared. The latter was then considered part of the induced drag, because its dependence on c_a is as to the square also. As a result, it was possible to introduce a substitute span with which the previously derived formulas could be analyzed.

2. THE PROFILE DRAG LAW

Now it is readily seen that the law for the profile drag contained in formula (1) cannot be carried into effect except in very few cases. To begin with, the occurrence of minimum profile drag at $c_a = 0$ is obviously precluded as far as cambered airfoils are concerned. One need only think of the conditions existing on greatly cambered profiles to realize this. With such profiles the flow, as is known, has already broken down on the bottom camber when $c_a = 0$, so that the polar reveals a break above $c_a = 0$. But owing to the rounded-off nose* it must be preceded by a gradual breakdown of the flow when - com-

*The validity is limited to profiles with rounded-off nose.

ing from high c_a values - approaching the c_a value of the lower break (fig. 2). Thus the conditions are similar to those encountered upon approaching the upper burbling point. Consequently, while there may exist a parabolic law for the dependence of profile drag on lift coefficient, the apex of the parabola for symmetrical wing sections, however, can only lie with $c_a = 0$. Dropping, in addition, the assumption of squared parabola, the general term for the profile drag then, is:

$$c_{w_{prof}} = c_{w_{prof_{min}}} + c\,(c_a - c_{a_{sym}})^n \neq c_{w_{prof_{min}}} + c\,(\Delta c_a)^n \qquad (2)$$

Hereby, $c_{a_{sym}}$ = c_a value at which the apex of the parabola lies

n = exponent of parabola

Δc_a = $c_a - c_{a_{sym}}$

c = constant

$c_{w_{prof_{min}}}$ = minimum profile drag coefficient lying at $c_{a_{sym}}$

The formula contains only the amount of the power.

It is now necessary to check whether the given term actually agrees with the given conditions, at least of normal wing sections, and for the most important flight range.

3. INVESTIGATION OF GÖTTINGEN AIRFOIL DATA REGARDING THE VALIDITY OF THE CITED PROFILE DRAG LAW

The writer, in collaboration with L. Maxen and F. Freytag, undertook the investigation of the validity of the law contained in formula (2) on a series of wing sections. In order to be able to embody the chosen airfoils in a system, the analysis was limited to Joukowski type and related airfoils, shown in figure 1 and table I. This work thus forms a complement to Schrenk's report (reference 3) and is equally confined to wind-tunnel tests. Even the method of defining the profile drag polars by

forming differences from the total drag obtained by weighing, and the induced drag known from theory was preserved in principle. One difference, however, which is of primary importance for the size of the profile drag coefficient and for the establishment of an experimental profile drag law, is that the calculation of the induced drag proceeds from a rectangular rather than an elliptical lift distribution. For equal aspect ratio $\frac{F}{b^2} = 1:5$,* there is, as known (reference 4), a 1.04 times induced drag with rectangular, as compared to elliptical, lift distribution. Thus at higher c_a the values for the profile drag would be lower than otherwise generally assumed. For this reason we added an increment of 2 percent to the induced drag, and the calculation was actually made with 1.06 times the induced drag obtainable with elliptical lift distribution. The reason for this increment was the fact that, according to pressure-distribution measurements on rectangular wings, the edges reveal high lift peaks, i.e., deviations from the theoretical rectangular lift distribution.

The thus obtained profile drag polars were then divided in a quota $c_{w_{prof_{min}}}$ not dependent on c_a and a quota $\Delta c_{w_{prof}}$ dependent on c_a (fig. 2). The next step was the determination of $c_{a_{sym}}$. Hereby it was observed that the quota dependent on c_a at high Δc_a values were agreeable as closely as possible because the instrumental errors during the division of the profile drag are comparatively smallest in these parts of the polars. The third step consisted of plotting on logarithmic scale the quota $\Delta c_{w_{prof}}$ against Δc_a.

---

*The fundamental measurements for the tests were made on normal wings of $\frac{F}{b^2} = 1:5$ aspect ratio.

TABLE I. Investigated Airfoils Similar to Joukowski Type Airfoils

Airfoil No.	$\frac{f}{l}$	$\frac{d}{l}$
410	0.0	0.145
494	.1	.0355
495	.1	.055
400	.105	.0583
496	.1	.084
497	.1	.113
430	.103	.113
498	.1	.142
413	.105	.145
500	.12	.055
502	.12	.142
656	.2	.148
657	.2	.148
523	.198	.165
652	.1965	.1665

4. RESULT OF INVESTIGATION

a) General result

The general result of the investigation of Joukowski type and related airfoils, which may be denoted as the "profile drag law", may be expressed as follows:

The profile drag polars for airfoils with thickness parameters $\frac{d}{l} \leqq 0.4$ and camber parameters $\frac{f}{l} \leqq 0.25$ may be replaced with cubical parabolas. The apex of the parabola for cambered airfoils lies above $c_a = 0$.

b) Magnitude of $c_{w_{prof_{min}}}$

The obtained $c_{w_{prof_{min}}}$ values for Joukowski and related airfoils are shown in figures 3 and 4 plotted against $\frac{d}{l}$ and $\frac{f}{l}$. During the determination of the values it was found that the profile drag polars occasionally yielded

only the values up to $\frac{f}{l} = 0.25$ because by definition $c_{w_{prof_{min}}}$ is to be the minimum value of the profile drag, which lies at $c_{a_{sym}}$. For greatly cambered airfoils $\left(\frac{f}{l} > 0.25\right)$ it was found, however, that the lower break of the polar lies above $c_{a_{sym}}$, as a result of which it was impossible to determine the magnitude of $c_{a_{sym}}$.

An examination of the curves manifests a linear relation between $c_{w_{prof_{min}}}$ and the airfoil thickness, valid up to about $c_{w_{prof_{min}}} = 0.018$, respectively, comprising the airfoils up to $\frac{f}{l} = 0.2$ and $\frac{d}{l} = 0.25$. Beyond $\frac{d}{l} = 0.25$ the $c_{w_{prof_{min}}}$ values rise considerably. The slope of the straight line $c_{w_{prof_{min}}} = f\left(\frac{d}{l}\right)$ is unaffected by $\frac{f}{l}$. The straight lines may be expressed with:

$$c_{w_{prof_{min}}} = f\,\frac{d}{l} = c_{w_{prof_{min}}\left(\frac{d}{l}=0.0\right)} + 0.044\,\frac{d}{l} \qquad (3)$$

The value of $c_{w_{prof_{min}}\left(\frac{d}{l}=0.0\right)}$ is not 0.0046 for non-cambered airfoils, as the extrapolation of curve $c_{w_{prof_{min}}\left(\frac{f}{l}=0.0\right)} = f\left(\frac{d}{l}\right)$ reveals. It would be 0.0055, according to measurements on a flat plate at $R = 4 \times 10^5$, the same at which the airfoil measurements were made. Of course, this figure is valid only under the premise of turbulence of boundary layer over the whole plate depth, an assumption which is perhaps not altogether complied with in the airfoil measurements.

The plotting of the $c_{w_{prof_{min}}}$ values against $\frac{f}{l}$ (fig. 4) discloses a parabolic relationship of the form

$$c_{w_{prof_{min}}} = c_{w_{prof_{min}}\left(\frac{f}{l}=0.0\right)} + \text{const}\left(\frac{f}{l}\right)^m \qquad (4)$$

A logarithmic diagram of the values gave a parabola exponent $m \approx 3$, a figure valid up to about $\frac{f}{l} = 0.225$. Beyond it, m increases consistently.

The values of the constants are found from table II.

TABLE II. Constants of Formulas (4) and (5) versus $\frac{d}{l}$

$\frac{d}{l}$	constant
0.0-0.2	~ 0.45
.25	~.50
.30	~.60
.40	~.90

Now $c_{w_{prof_{min}}}$ versus $\frac{f}{l}$ and $\frac{d}{l}$ may be approximated as

$$c_{w_{prof_{min}}} = 0.0046 + 0.044 \frac{d}{l} + \text{const}\ldots\left(\frac{f}{l}\right)^3 \qquad (5)$$

The formula is valid, as stated before, up to $\frac{d}{l} = 0.25$ and $\frac{f}{l} = 0.225$. Putting the constant for this range at 0.48, we obtain

$$c_{w_{prof_{min}}} = 0.0046 + 0.044 \frac{d}{l} + 0.48 \left(\frac{f}{l}\right)^3 \qquad (5')$$

as approximation formula.

c) The Magnitude of $\Delta c_{w_{prof}}$

$\Delta c_{w_{prof}}$ is, as previously explained, a function of $\Delta c_a = c_a - c_{a_{sym}}$, for which reason the determination of the magnitude of $c_{a_{sym}}$ formed the second step in the definition of the profile drag. However, in order to complete the discussion of the quotas of the profile drag first, it is deemed best to revert to the magnitude of $\Delta c_{w_{prof}}$ and thereby assume the magnitude of $c_{a_{sym}}$ to be known.

Figures 5a to 5f and 6a to 6f show as examples the logarithmic diagrams of the Δc_w values versus Δc_a for two series of regular Joukowski airfoils: once for constant thickness $\left(\frac{d}{l} = 0.1\right)$ and variable camber $\left(\frac{f}{l} = 0.0 \text{ to } 0.25\right)$ and then for constant camber $\left(\frac{f}{l} = 0.1\right)$ and variable thickness $\left(\frac{d}{l} = 0.0 \text{ to } 0.4\right)$. A straight line with 1:3 slope is drawn through the points. Naturally this method of plotting gives the points a more or less pronounced scatter because the instrumental errors now enter only in the Δc_a. The points for high Δc_a values have been particularly observed when drawing the straight lines. They lie quite well on the straight lines. Strictly viewed, the slope of the straight lines naturally fluctuates also, but the coordinated constant (intersection of straight line with the parallel to axis Δc_w at $\Delta c_a = 1.0$) of the chosen slope, affords a certain equalization.

The remaining figures may equally well be obtained with straight lines of 1:3 slope. All measurements, of course, are subject to the limitation that $\frac{f}{l}$ must not exceed 0.25.

The c constants of formula (2) defined as straight lines in logarithmic diagram, are shown in figures 7 and 8 for pure and modified Joukowski wing sections versus $\frac{f}{l}$ and $\frac{d}{l}$. There is a pronounced scatter which makes it difficult to obtain curves with very many test points, although it was quite satisfactory in isolated cases as, for example, in the plotting of c versus $\frac{f}{l}$ for $\frac{d}{l} = 0.1$, 0.15, and 0.3. The other curves were drawn accordingly, without regard to any marked, or perhaps, even one-sided scattering of the corresponding test points.

The plotting of the c constants against $\frac{d}{l}$ proximated hyperbolas, and against $\frac{f}{l}$ parabolas. Because of the pronounced scatter, no formal evaluation of the curves was attempted.

d. Magnitude of $c_{a_{sym}}$

The determination of this value is of particular significance insofar as it is possible theoretically to determine the location for infinitely thin airfoils, and it was found that this location was, as anticipated, in accord with that obtained by experiment. Further, it was established that, as regards $c_{a_{sym}}$, there exists a simple corelation for the airfoils of finite thickness.

Let us first examine the experimental values (figs. 9 and 10). Figure 9 shows that the $c_{a_{sym}}$ values for airfoils of equal camber plotted against $\frac{d}{l}$, may be approximately connected by straight lines. These lines are so much steeper as the camber is greater. The origin of the straight line in the ordinate axis is coincident with the point of $c_{a_{sym}}$ (obtained by extrapolation) for $\frac{d}{l} = 0.0$.

The extrapolation was made as follows: From the $c_{a_{theor}}$ and $c_{a_{exper}}$ diagrams plotted against α for the Joukowski airfoils, we took the conversion factors $\frac{c_{a_{exper}}}{c_{a_{theor}}}$ independent of α, and plotted them against the camber for $\frac{d}{l} = 0.05$ to 0.25 (fig. 11). The result was a set of parallelly displaced curves. It was assumed that this parallel shifting applied very likely to the curve for $\frac{d}{l} = 0$ also. For obvious reasons the origin of the curve for $\frac{f}{l} = 0$ had to be in point $\frac{c_{a_{exper}}}{c_{a_{theor}}} = 1$. With these values of the quotients the theoretically obtainable values of $c_{a_{sym}}$ for $\frac{d}{l} = 0$ then gave the corresponding experimental figure.

No definite statement may be made about the curves in figure 9 within range of $\frac{d}{l} > 0.4$, because of the lack of experimental data on airfoils of greater thickness. Consequently, the extrapolation of the straight line over $\frac{d}{l} = 0.4$ in figure 9, is not absolutely certain.

Figure 10 gives $c_{a_{sym}}$ versus $\frac{f}{l}$. According to it the rise at first is subsequently followed by a drop in the values within range of the tests for $\frac{d}{l} > 0.25$. Hence the recurrence of $c_{a_{sym}} = 0$ for the same profile thickness, once for $\frac{f}{l} = 0$ and again for $\frac{f}{l} > 0$.

Next it was attempted to establish one particular point on the airfoil to which the pertinent value of $c_{a_{sym}}$ could be somewhat coordinated.

An excellent point for cambered airfoils of zero thickness is the leading edge. In order to obtain the minimum profile drag the forward stagnation point must evidently lie in the leading edge because, selecting a point in the vicinity of the leading edge, the circulation of the leading edge, respectively the ensuing great velocities, would undoubtedly involve a much higher profile drag than with the so-called "shock-free entry" of the flow. Adding further the trailing edge in the known manner as rear stagnation point, the angle of attack of the airfoil and the corresponding c_a and $c_{a_{sym}}$ value (reference 5) is known according to the equally assumed as known results of the conformal transformation.

Passing to profiles of finite thickness, one might be tempted to assume that the forward stagnation point to which α_{asym} is coordinated, is coincident with the intersection of the profile contour and the extension of the skeleton line of the thick airfoil (profile with zero thickness and equal camber). But the design figure (fig. 12) shows that a substantially higher theoretical angle of attack belongs to this point (point 2); that is, a much higher lift also. On the other hand, according to figure 9, the $c_{a_{sym}}$ value decreases as the profile thickness increases. This signifies that the forward stagnation point of the cited intersection of skeleton line and profile contour (point 2 in fig. 12) moves forward (in direction of the arrow). Such a point of the profile is the intersection of profile contour and axis of abscissa (point 3 in fig. 12). We coordinated the same theoretical angle of attack to this point independent of $\frac{d}{l}$, although the corresponding lift coefficient still continues to rise,

albeit slightly, as a result of the increasing thickness of the profile. The pertinent c_a values for this point are included in figure 9.

As previously stated, there is no agreement between experimental and theoretical values for $\alpha_{theor} = const.$ For this reason the corresponding curves were not plotted in figure 10, although it contains the theoretical curve for $\frac{d}{t} = 0.0$.

Graphical determination of the actual position of the forward stagnation points by means of the α_{sym} values coordinated to the experimentally defined $c_{a_{sym}}$ values; that is, on the "generating circles" of the profiles as well as on the profile contours themselves, discloses these points in the design figures to again lie approximately on straight lines (figs. 13 and 14). The test points in the Z plane, that is, in the representation of the "generating circles" are best replaced with a straight line, whereas this is hardly possible for greater $\frac{f}{t}$ in the representation of the Joukowski airfoils. One obtains instead slightly cambered curves in the Z plane.

The straight lines containing the forward stagnation points in the representation of "generating circles" are steeper as the profile camber is greater. It ties up with the relationship existing between figure 9 and figures 13 and 14. But the advantage of the latter over figure 9 is their lucidity as well as the fact that the scattered test points may be closely replaced by straight lines through this method of representation. Only by computing the $c_{a_{sym}}$ values corresponding to these straight lines were the slightly cambered experimental curves of figure 9 and the experimental curves of figure 10 established.

Now the theoretical values may be obtained from the experimental for any thickness parameter with the quotients $\frac{c_{a_{exper}}}{c_{a_{theor}}}$ of figure 11, in the same manner as the $c_{a_{sym_{exp}}}$ for $\frac{d}{t} = 0.0$. The curves obtained in this fashion are shown as dashed lines in figures 9, 10, 13, and 14 for the profiles with maximum $\frac{f}{t}$ and $\frac{d}{t}$.

Figure 15 finally shows the pitch of the straight lines connecting the forward stagnation points of figures 13 and 14 plotted against the camber. The values diverge comparatively little from a parabola.

5. APPLICATION OF THE RESULTS TO THE PERFORMANCE CALCULATION OF AIRPLANE DESIGNS

In the numerical example hereafter, we show what differences occur in the magnitude of the most essential aerodynamic performance factors when the calculation is made with constant profile drag coefficient and when effected with profile drag coefficient dependent on lift coefficient. As example, we use a glider with non-twisted elliptical wings of 1:15 aspect ratio and constant profile; wing warping and profile change of outer wings shall be disregarded for reasons of simplicity. The chosen profile is a Joukowski airfoil with a thickness parameter $\frac{d}{l} = 0.125$, camber parameter $\frac{f}{l} = 0.15$, and wing span = 15 meters.

Figure 3 yields: $c_{w_{prof_{min}}} = 0.012$

Figure 11 " : $c = .0325$

Figure 13 " : $c_{a_{sym}} = .7$

As residual drag coefficient, we take

$$c_{w_R} = 0.0025$$

so that $c_{w_{s_{min}}} = .0145$

therefore, $f_{w_{s_{min}}} = .0145 \times 15 = 0.2175 \text{ m}^2$

Whence with point-by-point evaluation, the lift coefficient c_a :

With best criterion of climb at $c_{a_{st}} = 1.05$ (1.4325)

" " lift/drag ratio at $c_{a_\epsilon} = .80$ (0.826)

The criterion of climb $\frac{c_w}{c_a^{3/2}} = s$

With best criterion of climb at $s_{st} = \frac{1}{27.375} \quad \frac{1}{29.275}$

" " lift/drag ratio at $s_\epsilon = \frac{1}{25.475} \quad \frac{1}{25.84}$

The lift/drag ratio $\frac{c_a}{c_w} = \epsilon$

With best criterion of climb at $\epsilon_{st} = 26.8 \quad (24.55)$

" " lift/drag ratio at $\epsilon_\epsilon = 28.5 \quad (28.45)$

The conversion factors are:

$$\frac{c_{a_{st}}}{c_{a_\epsilon}} = 1.313 \ (1.734); \quad \frac{s_{st}}{s_\epsilon} = 0.93 \ (0.882)$$

$$\frac{\epsilon_{st}}{\epsilon_\epsilon} = 0.941 \ (0.8625)$$

The figures given in parentheses are the quantities obtained for constant parasite drag coefficient $c_{w_{s_{min}}} = 0.0145$ according to Schrenk (reference 1). The bracketed figures for the case of best lift/drag ratio differ very little from those corresponding to the actual course of the polar. But the figures for the best criterion of climb, on the other hand, reveal a perceptible difference, especially the c_a values. The c_a value of the best climb and ceiling factor ($c_{a_{st}} = 1.4325$) computed with constant profile drag coefficient, lies about 36.5 percent too high; that is, so high as to actually be quite close to the value of $c_{a_{max}} = 1.5$ of the airfoil.

Translation by J. Vanier,
National Advisory Committee
for Aeronautics.

REFERENCES

1. Schrenk, M.: Calculation of Airplane Performances without the Aid of Polar Diagrams. T.M. No. 456, N.A.C.A., 1928.

2. Schrenk, M.: A Few More Mechanical-Flight Formulas without the Aid of Polar Diagrams. T.M. No. 457, N.A.C.A., 1928.

3. Schrenk, O.: Systematic Investigation of Joukowsky Wing Sections. T.M. No. 422, N.A.C.A., 1927.

4. Betz, A.: Beiträge zur Tragflügeltheorie...Göttingen, 1919.

5. Schrenk, O.: Über die Theorie der Joukowsky-Profile. Z.F.M., June 28, 1927, p. 276.

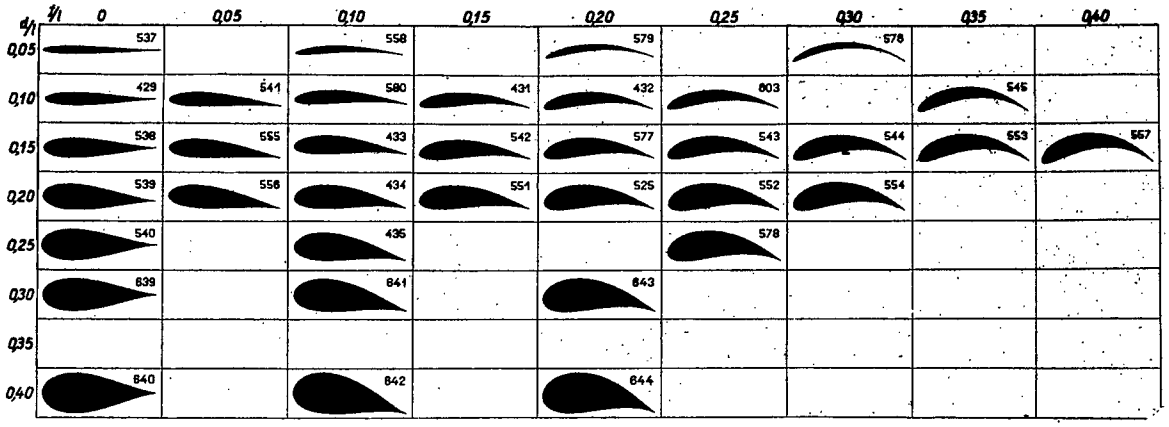

Figure 1.- Table of investigated Joukowsky airfoils.

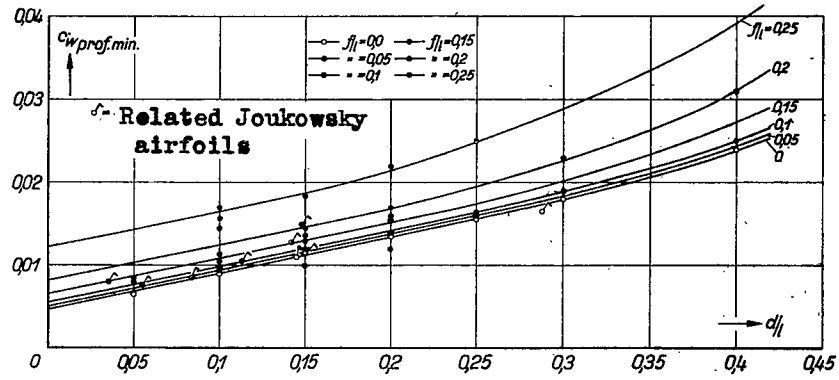

Figure 3.- Minimum profile drag versus thickness parameter (d/l)

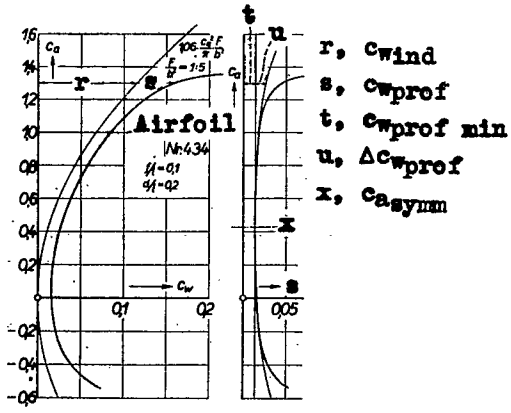

Figure 2.- Division of total drag of wing polars into drag quotas.

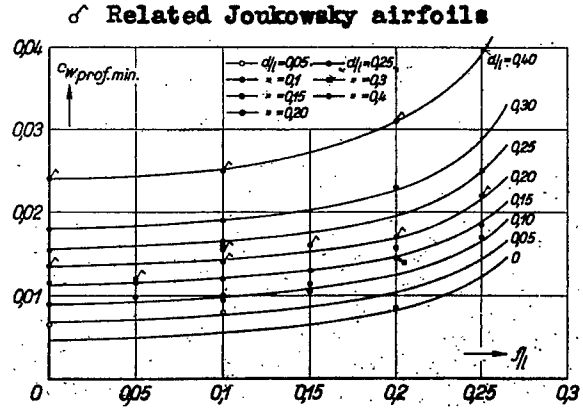

Figure 4.- Minimum profile drag versus camber parameter (f/l)

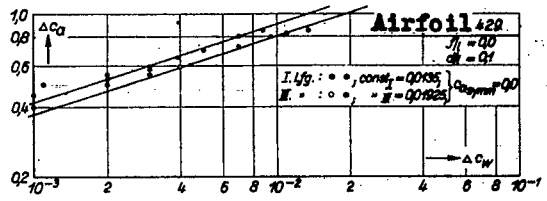

Figure 5a.

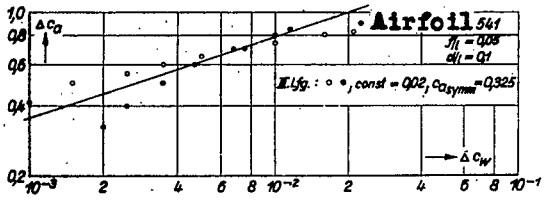

Figure 5b.

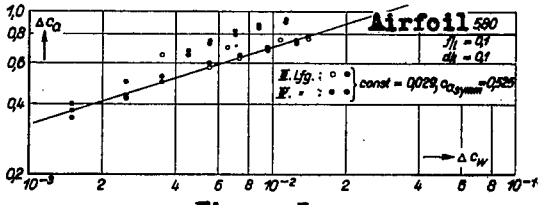

Figure 5c.

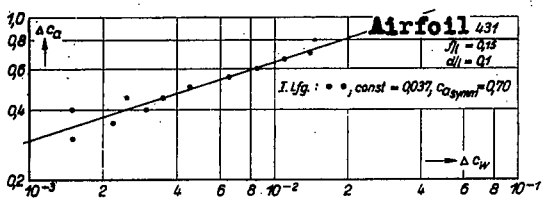

Figure 5d.

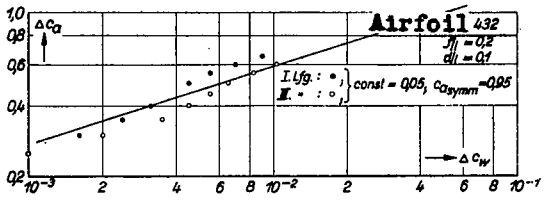

Figure 5e.

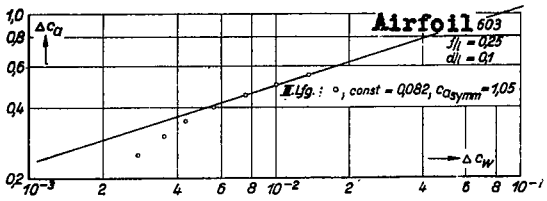

Figure 5f.

Figure 5(a-f).- Logarithmic plotting of profile drag quotas dependent on lift of Joukowsky airfoils with d/l = 0.1

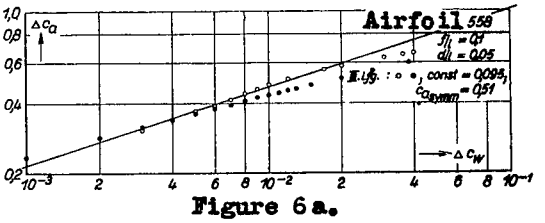

Figure 6a.

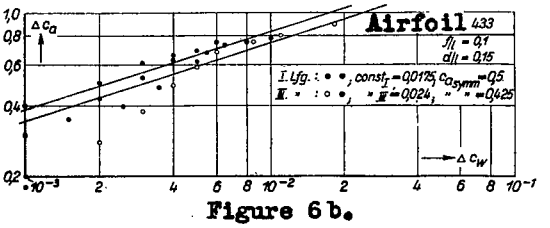

Figure 6b.

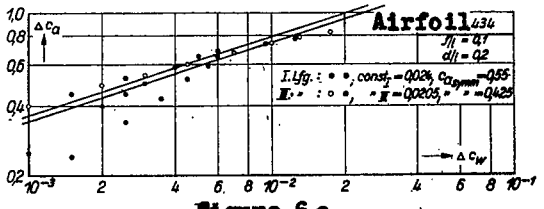

Figure 6c.

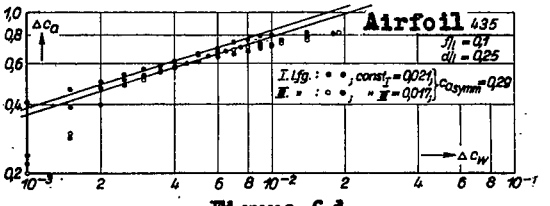

Figure 6d.

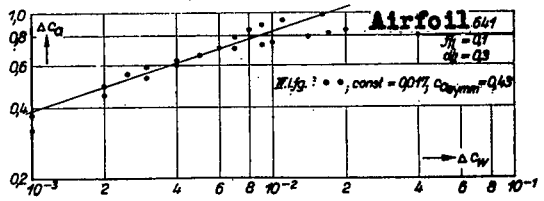

Figure 6e.

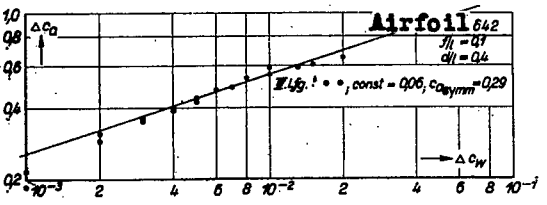

Figure 6f.

Figure 6(a-f).- Logarithmic plotting of profile drag quotas dependent on lift of Joukowsky airfoils with f/l = 0.1

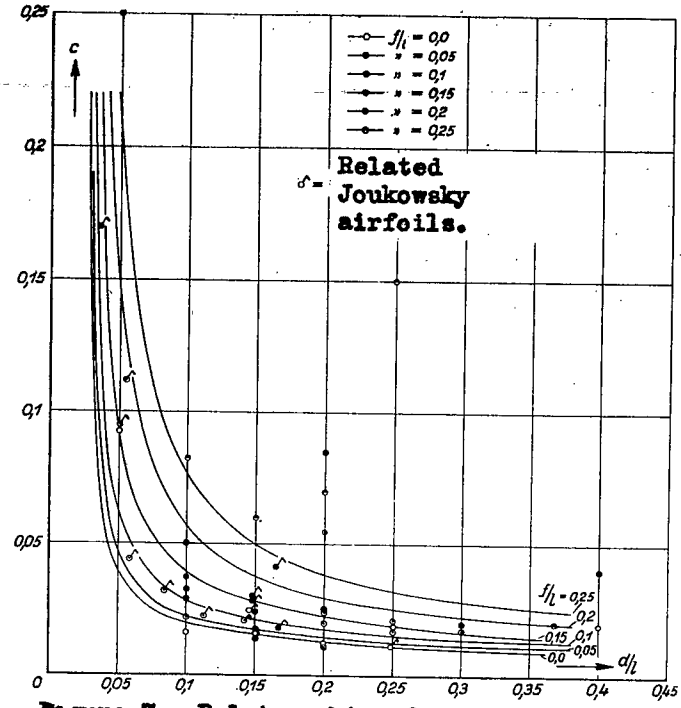

Figure 7.- Relationship of c constant of formula (2) to d/l .

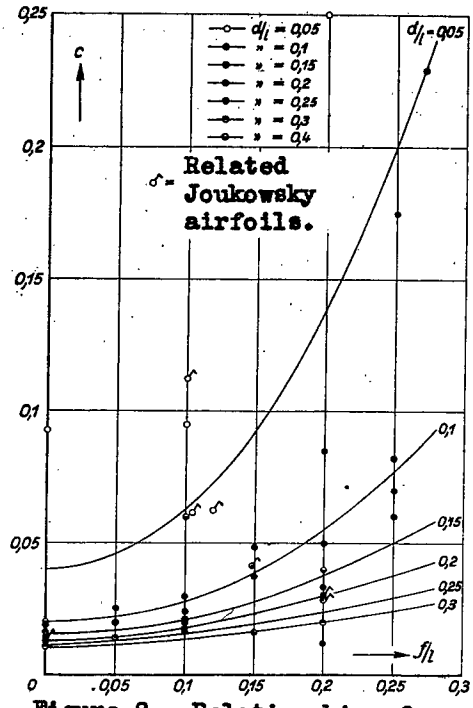

Figure 8.- Relationship of c constant of formula (2) to f/l .

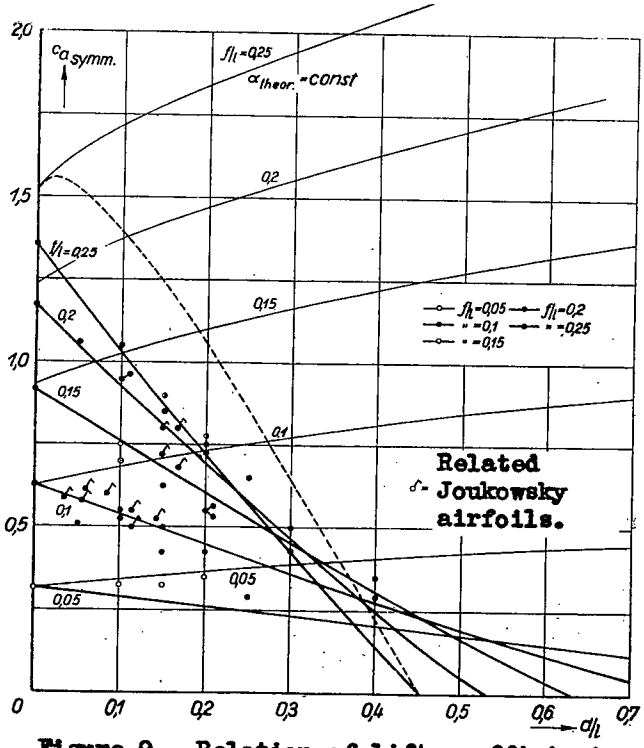

Figure 9.- Relation of lift coefficient for minimum profile drag to d/l .

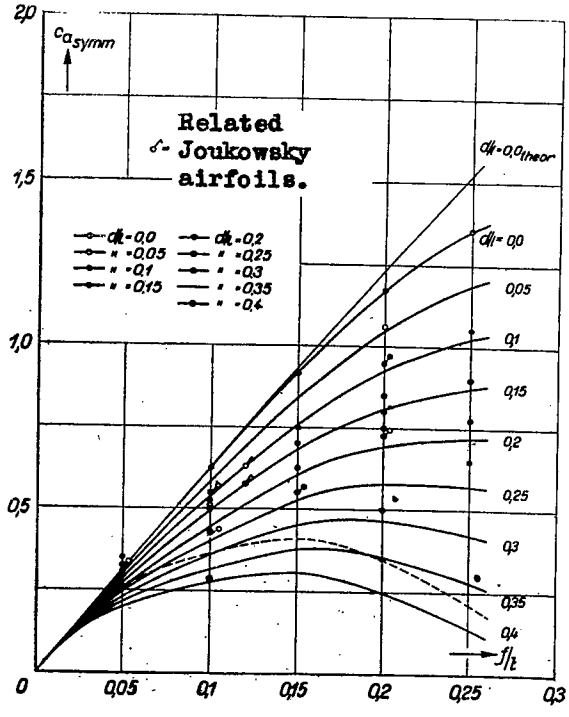

Figure 10.- Relation of lift coefficient for minimum profile drag to f/l .

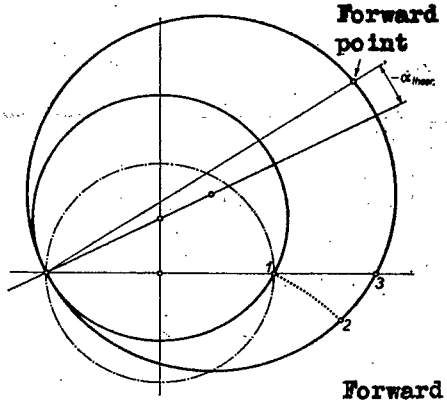

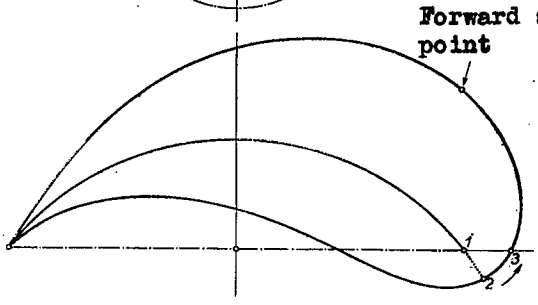

Figure 12.- Representation of travel of forward stagnation points corresponding to minimum profile drag with increasing profile thickness.

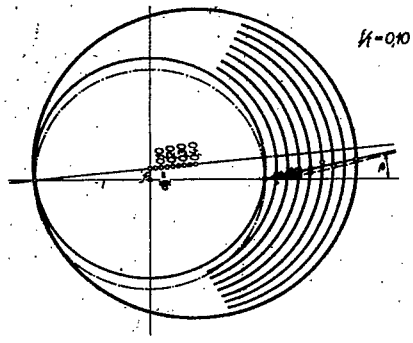

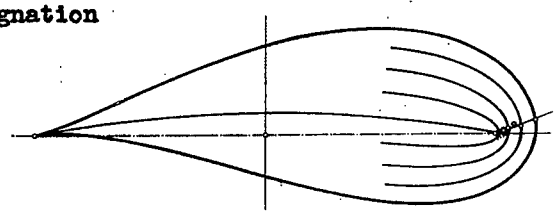

Figure 13.- Position of forward stagnation points for minimum profile drag on the "generating circles" and on the Joukowsky airfoils themselves (f/l = 0.1).

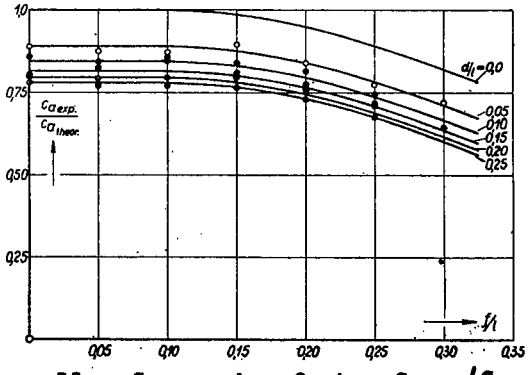

Figure 11.- Conversion factor $c_{a_{exp}}/c_{a_{theor}}$ of Joukowsky airfoils versus f/l.

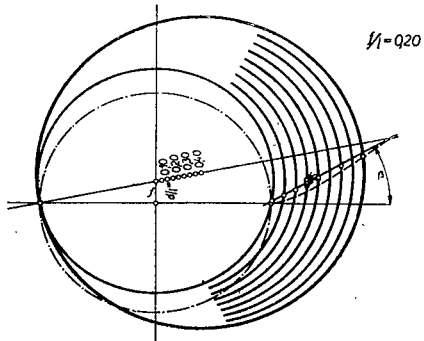

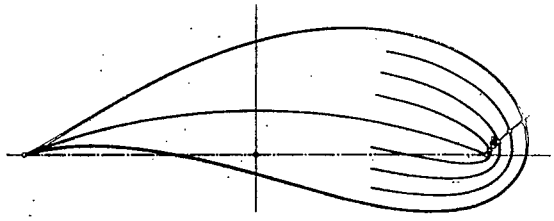

Figure 14.- Position of forward stagnation points for minimum profile drag on the "generating circles" and on the Joukowsky airfoils themselves (f/l = 0.2).

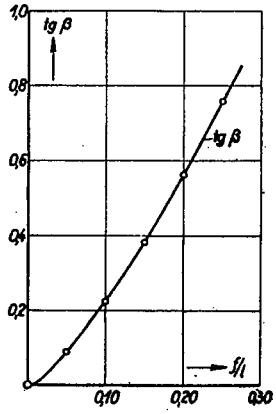

Figure 15.- Angle β of figs. 13 and 14 versus f/l.